AD-A109 700   NAVAL ACADEMY ANNAPOLIS MD   F/G 18/8
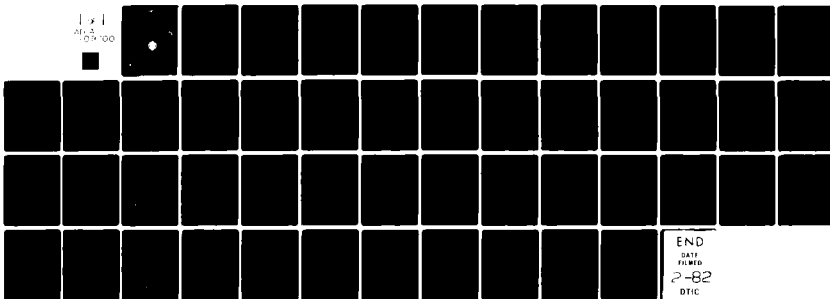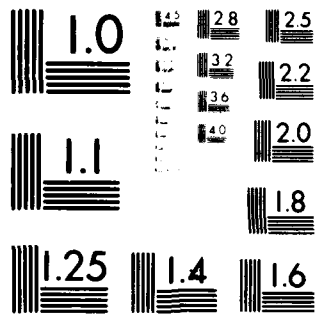   RADIATION EFFECTS ON TRANSMISSION IN OPTICAL FIBER SYSTEMS.(U)
                JUN 81   W H HILARIDES
UNCLASSIFIED   USNA-TSPR-110   NL

END
DATE
FILMED
2-82
DTIC

MICROCOPY RESOLUTION TEST CHART

NATIONAL BUREAU

LEVEL

(21)

A TRIDENT SCHOLAR
PROJECT REPORT

NO. 110

"RADIATION EFFECTS ON TRANSMISSION
IN OPTICAL FIBER SYSTEMS"

UNITED STATES NAVAL ACADEMY
ANNAPOLIS, MARYLAND
1981

82 01 15008

~~//. .. --T. . -11~~

REPORT DOCUMENTATION PAGE		READ INSTRUCTIONS BEFORE COMPLETING FORM
1. REPORT NUMBER U.S.N.A. - TSPR; 110 (1981)	2. GOVT ACCESSION NO. AD-A20	3. RECIPIENT'S CATALOG NUMBER
4. TITLE *(and Subtitle)* RADIATION EFFECTS ON TRANSMISSION IN OPTICAL FIBER SYSTEMS.		5. TYPE OF REPORT & PERIOD COVERED Final: 1980/1981
		6. PERFORMING ORG. REPORT NUMBER
7. AUTHOR(s) William Hunter Hilarides		8. CONTRACT OR GRANT NUMBER(s)
9. PERFORMING ORGANIZATION NAME AND ADDRESS United States Naval Academy, Annapolis.		10. PROGRAM ELEMENT, PROJECT, TASK AREA & WORK UNIT NUMBERS
11. CONTROLLING OFFICE NAME AND ADDRESS United States Naval Academy, Annapolis.		12. REPORT DATE 2 June 1981
		13. NUMBER OF PAGES 47
14. MONITORING AGENCY NAME & ADDRESS(if different from Controlling Office)		15. SECURITY CLASS. (of this report) UNCLASSIFIED
		15a. DECLASSIFICATION/DOWNGRADING SCHEDULE

16. DISTRIBUTION STATEMENT *(of this Report)*

This document has been approved for public release; its distribution is UNLIMITED.

17. DISTRIBUTIO.. STATEMENT *(of the abstract entered in Block 20, if different from Report)*

This document has been approved for public release; its distribution is UNLIMITED.

18. SUPPLEMENTARY NOTES

Accepted by the U. S. Trident Scholar Committee.

19. KEY WORDS *(Continue on reverse side if necessary and identify by block number)*
Neutron irradiation
Fiber optics

20. ABSTRACT *(Continue on reverse side if necessary and identify by block number)*

    A study was done of the effects of 14.7 Mev neutrons on transmission in optical fibers. This study was done with monochromatic light in the spectral range from 700 to 1700 nanometers. Of the fibers studied, two were high purity silica fibers. An important result of the study was that the radiation induced damage was wavelength related. The induced damage decreased rapidly as the wavelength increased from 800 to 1100 nanometers, with minimal damage noted above 1300 nanometers. This trend was due primarily to the energy levels of
(OVER)

CONTINUED

traps formed as the bombarding neutrons broke bonds within the silica. Several other interesting trends were noted. First, the water content of the fiber affected the amount of induced damage. Second, the method by which the fiber was made affected the damage levels. Third, the dopant used affected the damage levels. These trends deserved further study, but because the data base was so small, more specific conclusions were not possible.

0 - 0

Accession For

NTIS CRA&I	☑
DTIC TAB	☐
Unannounced	☐
Justification	

By
Distribution/
Availability Codes

Dist	Avail and/or Special
A	

"RADIATION EFFECTS ON TRANSMISSION

IN OPTICAL FIBER SYSTEMS"

A Trident Scholar Project Report

by

Midshipman First Class
William Hunter Hilarides
Class of 1981

U. S. Naval Academy

Annapolis, Maryland

Associate Professor Richard L. Johnston,
Physics Department

Accepted for Trident Scholar Committee

Chairman

2 June 1981
Date

ABSTRACT

A study was done of the effects of 14.7 Mev neutrons on transmission in optical fibers. This study was done with monochromatic light in the spectral range from 700 to 1700 nanometers. Of the fibers studied, two were high purity silica fibers, and two were Germanium doped core silica fibers. An important result of the study was that the radiation induced damage was wavelength related. The induced damage decreased rapidly as the wavelength increased from 800 to 1100 nanometers, with minimal damage noted above 1300 nanometers. This trend was due primarily to the energy levels of traps formed as the bombarding neutrons broke bonds within the silica. Several other interesting trends were noted. First, the water content of the fiber affected the amount of induced damage. Second, the method by which the fiber was made affected the damage levels. Third, the dopant used affected the damage levels. These trends deserve further study, but because the data base was so small, more specific conclusions were not possible.

TABLE OF CONTENTS

INTRODUCTION

Optical fibers are being utilized in industrial, communications, and military applications with ever increasing frequency. The use of these fiber systems without studying their response to ionizing radiation can have grave consequences, especially in military applications. Efforts to radiation harden optical systems by the military, as well as the space program and the communications industry, has helped to broaden our knowledge of the effects of ionizing radiation in optical fibers and many other materials.

Fiber optic technology has progressed to the point that very pure silica and specifically doped silica fibers are being produced at a reasonable cost. These fibers have the lowest natural attenuation in the 800-1300 nanometer range, which includes the near infrared region of the electromagnetic spectrum. Laser diodes, semiconductor light emitting diodes, and photodiodes are all being developed which operate in the near infrared region. A system operating in the near infrared range capitalizes on the minimization of natural attenuation and also a minimization of dispersion for many fibers. Examples of semiconductor devices now commercially available are a GaAlAs light emitting diode and photodiode, which operate at 850 nanometers, and a GaInAsP

light emitting diode and photodiode which operate at 1300 nanometers.

The shift to the near infrared wavelengths by the optics industry is the driving force behind this study. Several studies have been done to observe the effects of neutrons on transmission in visible frequencies, and also studies that utilized gamma or electron radiation.[1] But this study is the first on the effects of neutrons on transmission in the important near infrared region. Although the results of this study are not totally conclusive about the subject, the results provide considerable insight into the damage trends and the mechanisms describing these trends.

THEORY

The theory explaining waveguides for electromagnetic radiation has been understood for many years. But only until advances in chemistry and solid state physics have led to the production of ultrapure silicas, has the use of optical waveguides become a feasible option to standard electrical systems. As technology has progressed, the natural attenuation of the fibers has been reduced, allowing greater repeater distances. These advances have allowed fiber systems to compete on an economic level with electrical systems.

A step index optical fiber transmits light by the simple process of total internal reflection. A fiber is designed so that the core of the fiber has a higher index of refraction than the outer coating, known as the cladding.(Fig. 1).
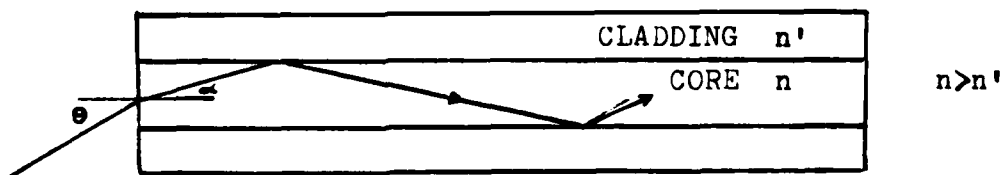

CLADDING   n'

CORE   n $n > n'$

Fig. 1 Step Index Fiber

Photons striking the end of the fiber at angle θ are bent towards the normal as described by Snell's Law, which can

be stated in the following manner:

$$(n_{air})\sin \theta = (n_{fiber})\sin \alpha$$

Total internal reflection occurs for all light hitting the
core-cladding interface with an angle α_{crit} such that:

$$\alpha_{crit} = \cos^{-1}(n'/n)$$

Thus the light inside the fiber is reflected from boundary
to boundary down the length of the fiber. The light there-
fore travels the distance of the fiber with very little loss
in intensity.[2]

Defects in the short range crystal lattice structure
of silica (which is amorphous in the long range) hinder
the transmission of light through the fiber. Defects of
various types can cause the light to scatter or can absorb
the photons. Some of the defects are inherent in the fibers
and can be generalized into several important categories.
These categories are:

       1. Impurity defects.

       2. Vacancy defects.

       3. Interstitial defects.

An impurity defect is a molecule other than a silicon
dioxide filling a lattice point. This molecule can cause
scattering because of its size or shape, or it can cause
absorption because of extra bonds that are created or left
unfilled. It is very difficult to get all of the impurities

out of the silica because of the methods of making the fibers.
Water and metal ions are common impurities found in fibers,
and the quality of many fibers can be measured by the per-
centage of impurities.

Vacancy defects are missing atoms in the lattice struc-
ture. A missing atom causes an interruption in the periodic
structure of the lattice, which can cause scattering of the
light. A vacancy is usually filled with one or more dangl-
ing bonds, because a vacancy usually means that several
bonding orbitals are not filled. These dangling orbitals
act as traps for electrons and holes, which can cause ab-
sorption bands in the fiber.[3]

The third type of defect, and interstitial defect, is
an extra molecule which sits at a point in the lattice which
is not usually occupied. An impurity molecule is the most
common type of interstitial defect, and can cause loss in
two ways. Because it is an interruption in the lattice
structure, the defect can cause scattering. The intersti-
tial molecule may also have unfilled orbitals, allowing it
to absorb the light. All of the defects combine to affect
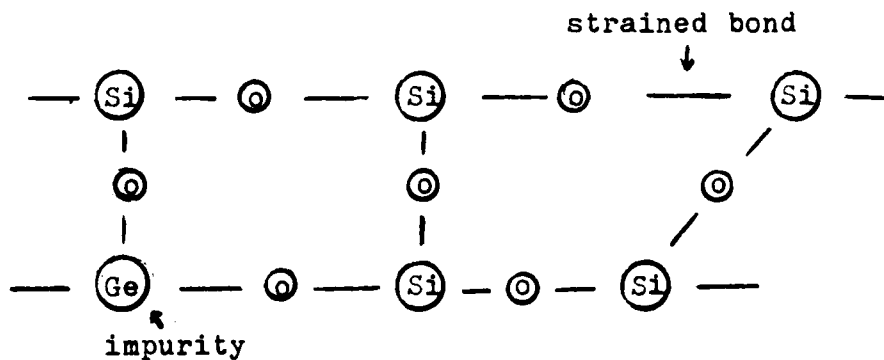the efficiency of the fiber as an optical waveguide.

An impurity defect can also be a desirable phenomenon.
When a silicon dioxide molecule is replaced by a germanium
dioxide molecule on a lattice point, the resultant crystal
is very similar in stability to a pure silica, but with
slightly different characteristics. One characteristic

commonly affected is the index of refraction. The process
of adding impurities, known as doping, can be used to vary
the index of refraction of the glass for the creation of
very specialized fibers. Many other benefits can be derived
from using dopants as well..

Silicon dioxide has a tetrahedral structure, but can
be modelled in two dimensions in the following manner:
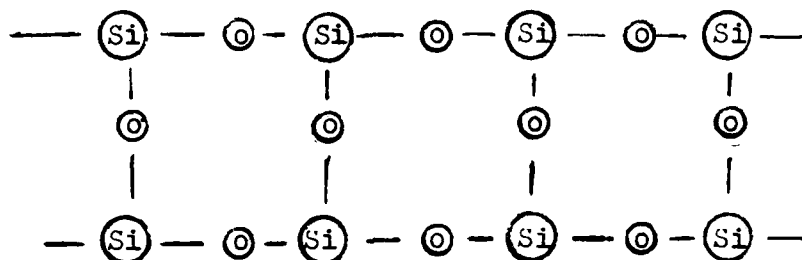
This model is an idealized lattice, and as was mentioned
before, only applies to short range order, but it is nec-
essary to use this model for theoretical discussion. Even
with the short range order, one is more likely to find the
crystal structure interspersed with impurities and strained
bonds:

When a strained bond is formed, it can be broken to create what is known as a color center. When the bond is broken, the crystal relaxes away from the broken bond, leaving a gap with dangling bonds:

broken bond

— (Si) — (O) — (Si) — (O)⁻   + (Si) —

    | |
   (C)   (O)   (O)
    | |
— (Ge) — (O) — (Si) — (O) — (Si) —

In this gap is a dangling oxygen orbital, which acts as a hole trap. The silicon also has an extra positive charge, which acts as an electron trap. When the silicon traps an electron, the fibers absorption in the ultraviolet range is increased. When the oxygen traps a hole, the range of absorption is in the visible spectral region.

The absorption mechanism can be understood using the band theory for solids.[4] The conduction band for pure silica is approximately nine electron volts above the valence band. This large energy gap means that silica is an insulator, and the size of the gap prevents normal lattice electrons or holes from absorbing optical photons. But the trapped hole and the trapped electron described above populate the energy gap with defect energy levels. The prescence of these levels allows transitions of much lower energies (Fig. 2).
The defects which produce energy levels in the gap are aptly

Pure Silica Energy Gap

9ev

Defect Levels in the Energy Gap

9ev _Defect_Levels_
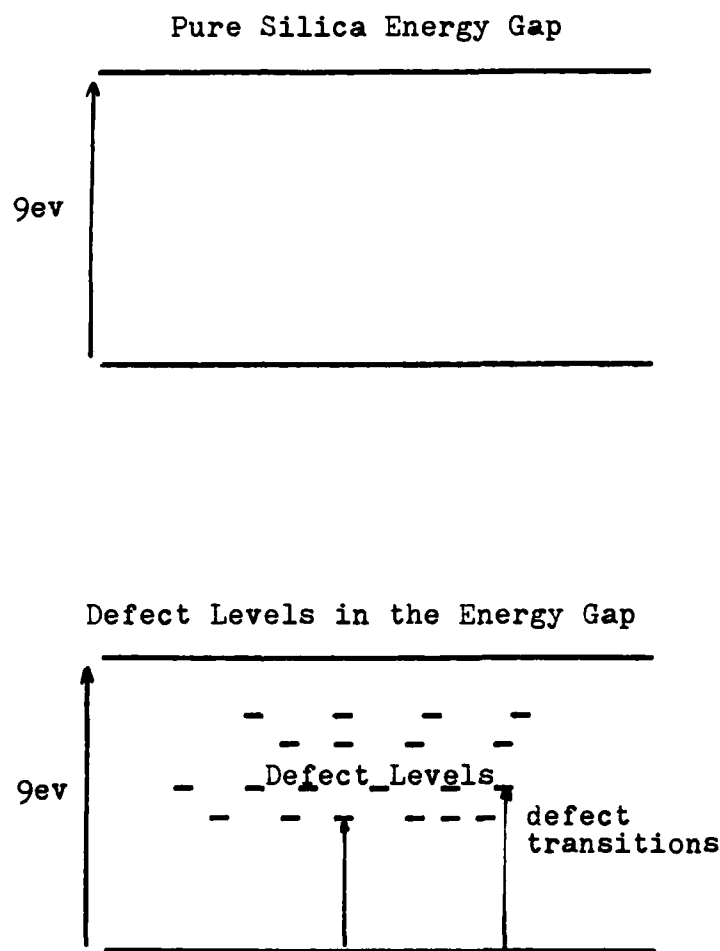
defect
transitions

Figure #2

Energy Level Diagrams

named "color centers", because they cause specific frequencies of light to be absorbed, giving the crystal color.

It has been discovered that ionizing radiation causes a dramatic increase in the number of color centers normally present in many fibers.[5] 14.7 mev neutrons, of the type used in this experiment, cause defects in the silica by two mechanisms;

      1. Collisions with molecules.

      2. Interactions with bonds.

In the first case, the energetic neutron collides with an atom, and in an elastic collision, displaces the atom from its lattice point. This creates a vacancy and an interstitial defect, both of which contribute defect energy levels to the energy gap. The second interaction usually occurs between the neutron and a bond which is abnormal, such as a strained bond. The interacting neutron causes the bond to break, allowing crystal relaxation and the creation of color centers as described earlier.

The radiation induced color centers all contribute defect levels to the energy gap. Because these energy levels can be characterized by their cause, the color centers are going to be concentrated at certain frequencies. The fact that these color centers are concentrated implies that the damage induced in the fiber is wavelength related. Therefore, if the concentrations are studied, a radiation hardened system can be designed using the wavelengths where the

number of radiation induced color centers is a minimum.

This study of radiation damage in certain fibers was done in the spectral range from 700 to 1700 nanometers for several reasons. First, the inherent loss for most fibers reaches a minimum in this range.[6] Second, the dispersion curve for most fibers tends towards a minimum in this region as well. Dispersion is the spreading out in time of a light pulse as it travels the length of the fiber. Dispersion is an important characteristic which limits the data rate at which a fiber optic system can operate. A fiber operates at maximum efficiency at the point where both the natural loss and the dispersion curves are minimized. For many fibers, this point is in the near infrared region of the spectrum.[7] Because of these trends, most of the fiber optics industries' research is being done to develop transmitters and detectors which operate in the 800 to 1300 nanometer range.

APPARATUS

The basic apparatus used in the experiment was a simple one. A Baush and Lomb scanning monochromator and a microscope objective were used to focus monochromatic light into the end of the fiber. A Rolfin frequency programmable chopper was used to pulse the signal before it entered the fiber, which was typical of a fiber optic system. The output of the fiber was shone on the germanium photodiode, which developed a potential proportional to the intensity of light striking it. This signal was then fed into a Princeton Applied Research lock-in amplifier along with a reference signal from the frequency controller of the chopper. The output of the lock-in amplifier was a D.C. signal proportional to the intensity of the light transmitted by the fiber. This signal was then put into a strip chart recorder, which produced a plot of the relative intensity transmitted by the fiber versus wavelength as the monochromator was rotated.

The original apparatus was set up to take data in the following manner:

1.) A full transmission spectrum (700 to 1700 was taken before irradiation.

2.) The monochromator was set on a specific wavelength and a plot of dB loss was made versus time.

3.) A post irradiation spectrum was completed

> to measure the total loss in intensity for
> the entire irradiation.

The data runs from this apparatus were difficult to handle
in strip chart form, so a major modification was made of the
apparatus.

A Transera analog-to-digital converter and a Textronix
4051 computer, which were designed to work in conjunction,
were added for data taking. With these additions, the data
taking apparatus was much more accurate (Fig. #3). A timer,
also designed by Transera for the 4051, was used to trigger
the computer to sample the output of the lock-in amplifier
at a certain interval. Because the monochromator was rota-
ted by a D.C. motor, the data correlation between intensity
runs depended on the constant speed of the motor and on how
accurately the experimenter could activate the computer
program as the monochromator passed 700 nanometers.

Three fibers were run on this apparatus, and the data
runs are included in Appendix #1. This data yeilded very
little information for three major reasons. They were:

> 1. The difficulty in lining up the before
> and after irradiation graphs for correlation.
>
> 2. The short lengths of fiber used.
>
> 3. The low neutron flux through the fiber.

At this point in the experiment, the entire apparatus
was redesigned to correct the difficulties. To remedy the
first problem, the D.C. motor used to move the monochromator
was replaced by a stepper motor. To best utilize the stepper

Figure #3
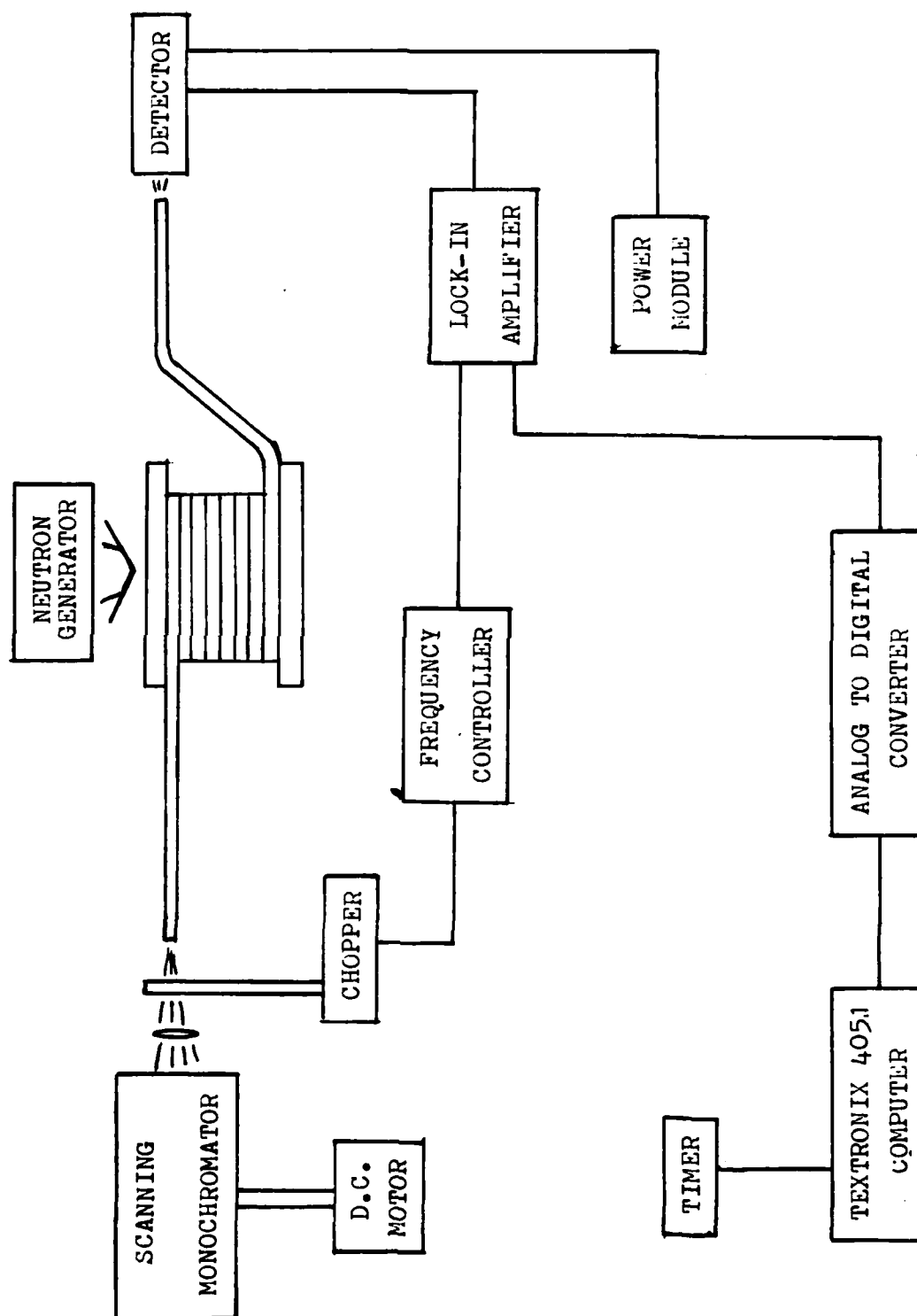
motor, a control package was designed and built to step the motor at the command of the computer. This was done using a hexadecimal output from the Textronix 4051 computer. The basic package was:

4051 COMPUTER	HEXIDECIMAL OUTPUT	AMPLIFIER	STEPPER I.C. CONTROL	STEPPER MOTOR
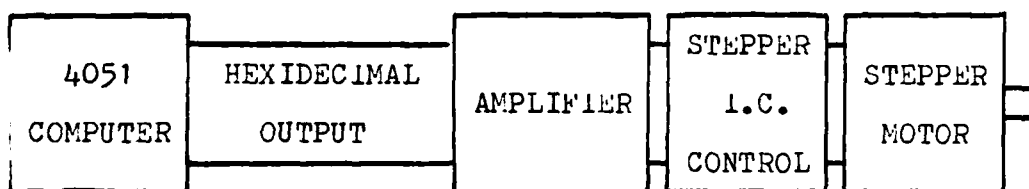
The use of the stepper motor allowed the exact selection of wavelength and also created the ability to return the diffraction grating to the exact starting point before beginning each intensity run.

Because of the holding coils present in the stepper motor, the monochromator diffraction grating was held tightly in place while the analog to digital converter sampled the detector output. This final apparatus had two major advantages. First, the 4051 computer controlled the entire data taking apparatus during a run, and second, the stepper motor allowed a very accurate wavelength discrimination. The tolerance of the motor was given as $\pm$ 30 minutes on a 7.5 degree step. Since each step represented .42 nanometers, the discrimination of the motor set up was on the order of $\pm$ .03 nanometers, which was an order of magnitude more accurate than the discrimination of the grating that was used. The final apparatus is diagrammed in Fig. #4.

Figure #4
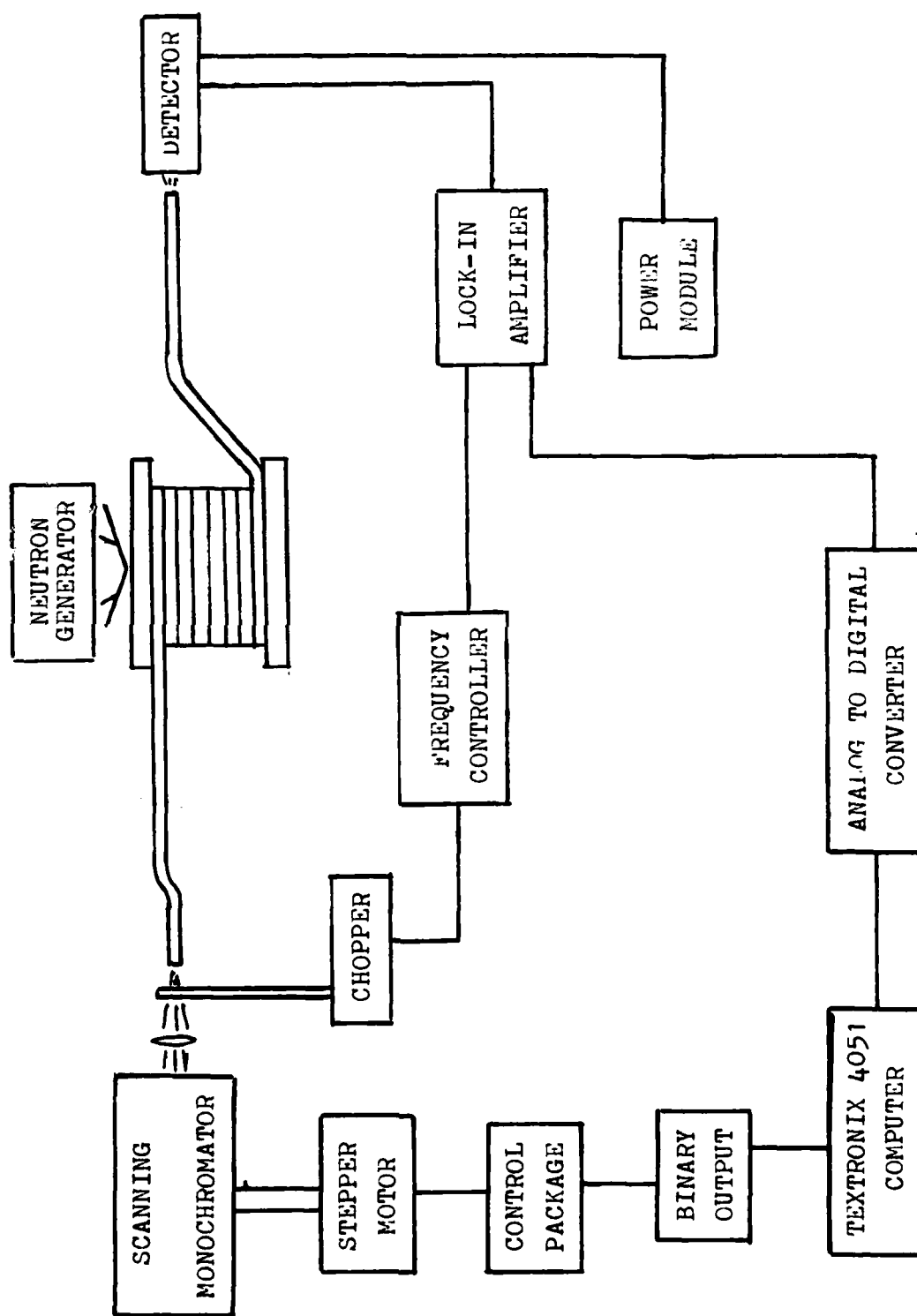
To improve the data further, a study was done to maximize the neutron flux through a spool holding approximately 100 meters of fiber. 100 meters of fiber was a much greater length than had been used earlier, and the length was increased to improve the data. A computer program was written to numerically integrate the neutron flux through various sizes of spools. The distance from the neutron generator was also calculated so as to give the maximum flux through the fiber. The model of the spool, the computer program and the results are all included in Appendix #2. The results of this study were then used to design the spools and the four fibers to be studied were wound on these spools.

EXPERIMENT

The resultant intensity curves for the initial fiber
runs, which were taken on the apparatus in figure #3, are
included in Appendix #1. These graphs yeilded very little
useful information and were the driving force behind the
redesign of the apparatus.

The four final data runs are included in Appendix #2.
For these runs, labratory conditions were kept as stable
as possible. All of the equipment, especially the white
light source and the germanium detector, was kept on through-
out the irradiation runs. This was important because of
warmup instabilities that had been noticed in the earlier
experiments. All of the data runs were completed in the
afternoon, with the neutron generator operating for one hour.
The entire apparatus was turned on and allowed to warm up
for at least three hours before starting the irradiation.

After the warmup period, and as the neutron generator
was coming onto the line, an undamaged fiber transmission
spectrum was completed. This run was to be the reference for
the damage caused by the neutrons. This run was completed
with all electrical equipment on but without neutron flux.
This was done to prevent line voltage spikes from upsetting
the detector. A spike had been noted in the earlier

experiments. Continuing the data run, the white light source
was then blocked off from the monochromator, preventing
light from entering the fiber, and the neutron radiation
was turned on.

At fifteen minute intervals the computer was activated,
causing the stepper motor to step forward 1200 steps (1000
nanometers), sampling the detector output at each step.
The computer program, listed in Appendix #4, then stepped
the motor backward 1200 steps to the exact starting position
of the diffraction grating, insuring repeatability of wave-
length. The data from each interval spectrum run was placed
on magnetic tape in separate files, and the five spectrum
transmission runs were completed for each fiber. The curves
from this section are included in Appendix #3.

Recovery transmission spectra were taken for one fiber,
a Quartz & Silice high purity silica fiber. These spectra
were taken on fifteen minute intervals after the radiation
was turned off. These runs are included in Appendix #5.

The data files taken in the data runs were transferred
from the magnetic tape to the Naval Academy's Dartmouth Time
Sharing System computer, where they could be accessed to
on line programs. Using several file manipulating programs,
the data points were correlated with specific wavelengths,
and all of the runs for a specific fiber were plotted to-
gether to produce the graphs included in Appendix #3.

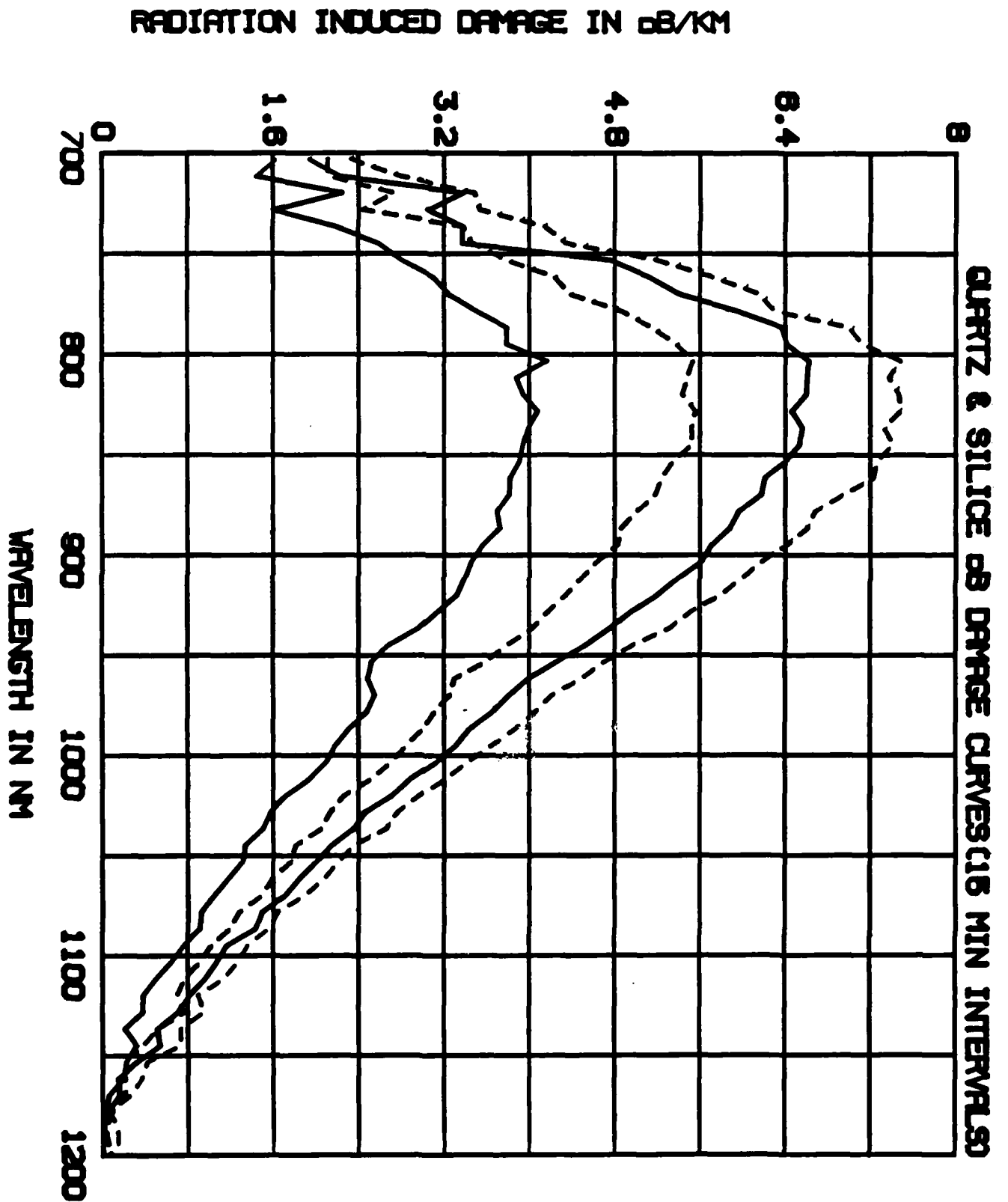Because the intensity curves are not useful in analyzing

data, the data was again manipulated to take the induced damage in decibels, from the intensity curves using the following formula:
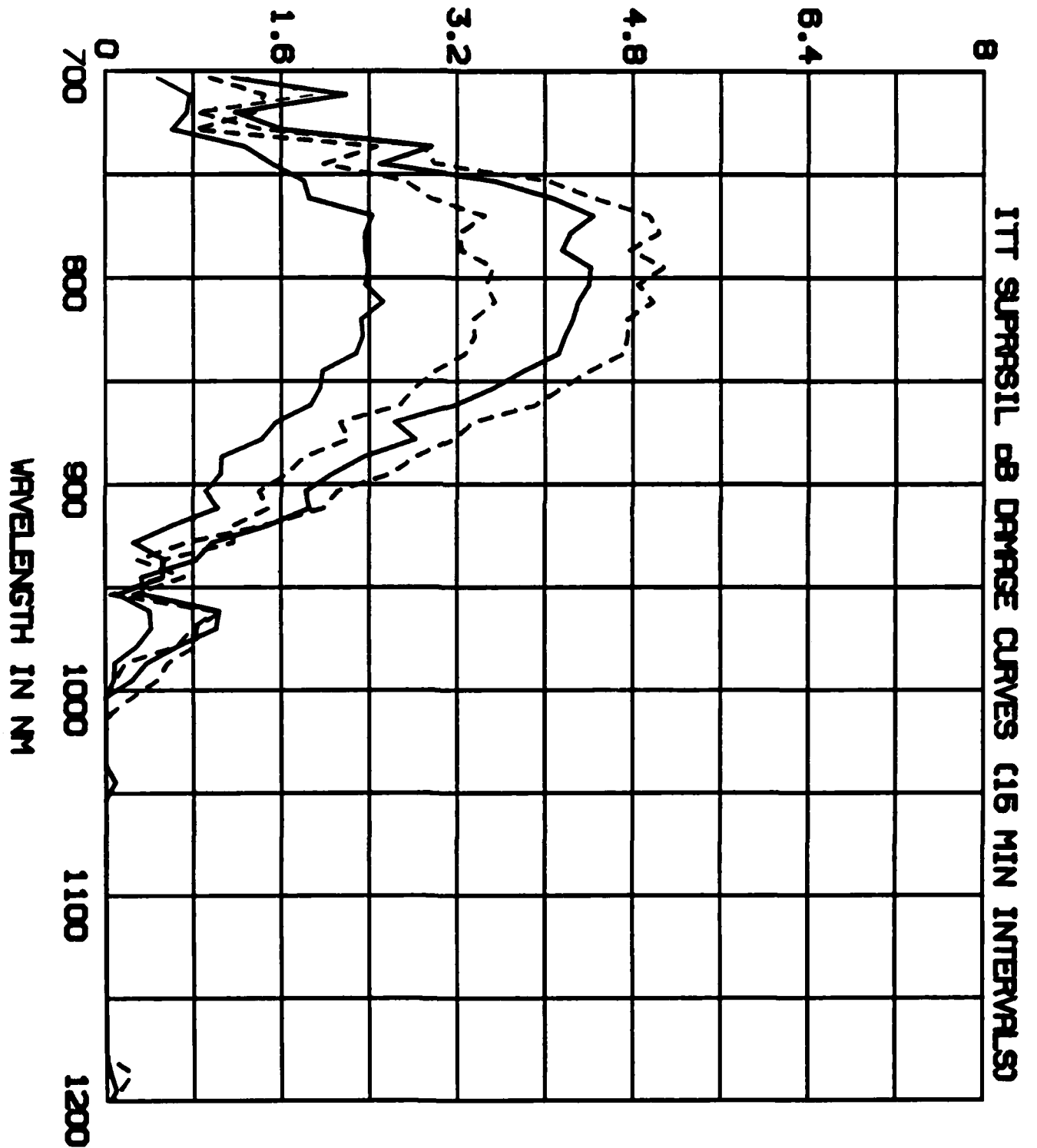
$$INDUCED\ DAMAGE(dB)=(-10)\ln(I/\ I_{ref})$$

These curves were then plotted together to yield a plot of the induced dB damage versus wavelength for the fifteen, thirty, forty-five and sixty minute runs. These graphs are included in the "results" section and are very informative about the amount of damage and rate of damage for various fibers.
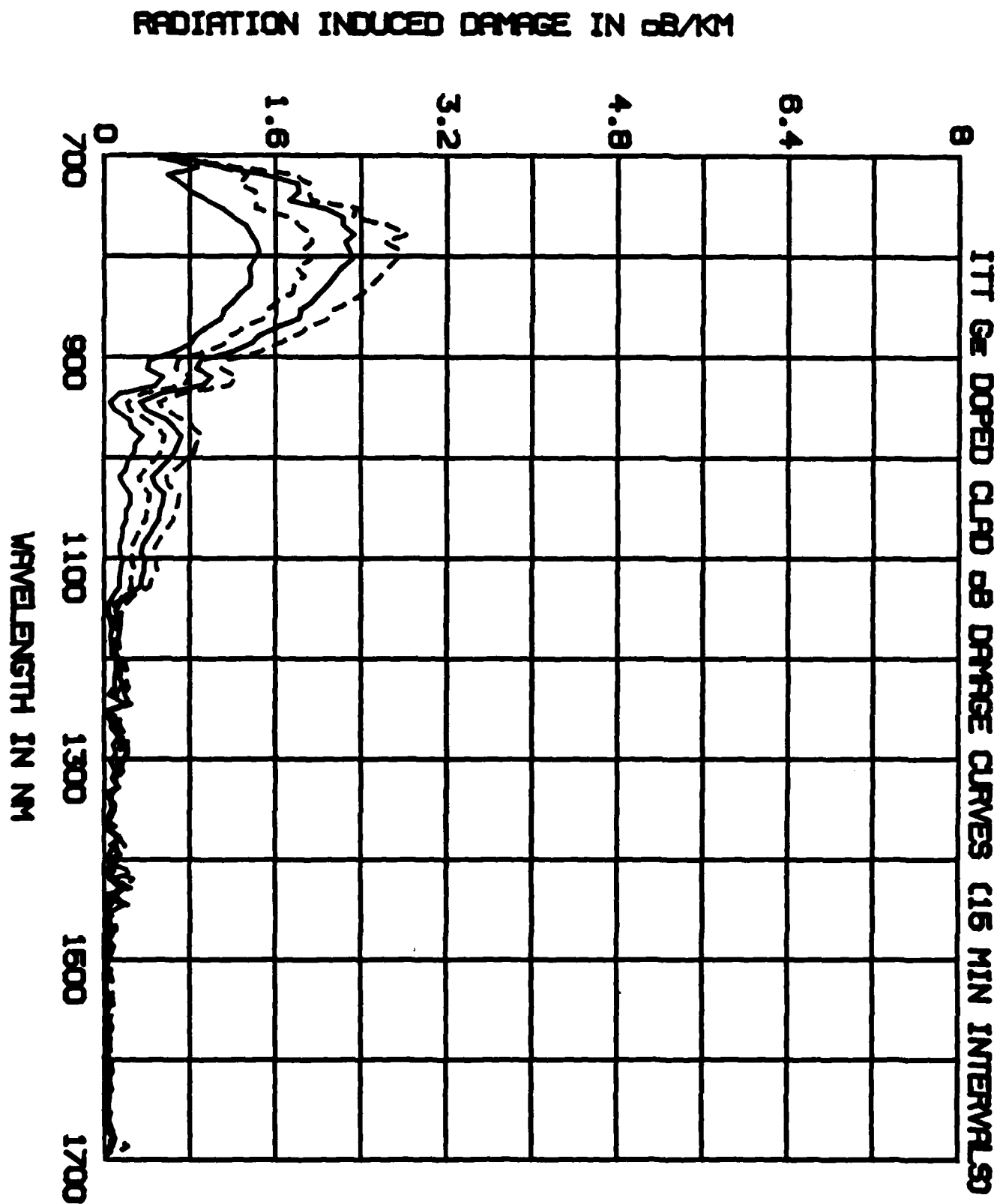
RESULTS

The next four pages are the graphs of the radiation induced damage measured in decibels for the four fibers that were tested in the final phase of the project. The curves represent the fifteen, thirty, forty-five and sixty minute damage levels for the irradiation run. The trend of damage is increasing, and the fifteen minute curve is always the bottom one on each plot.
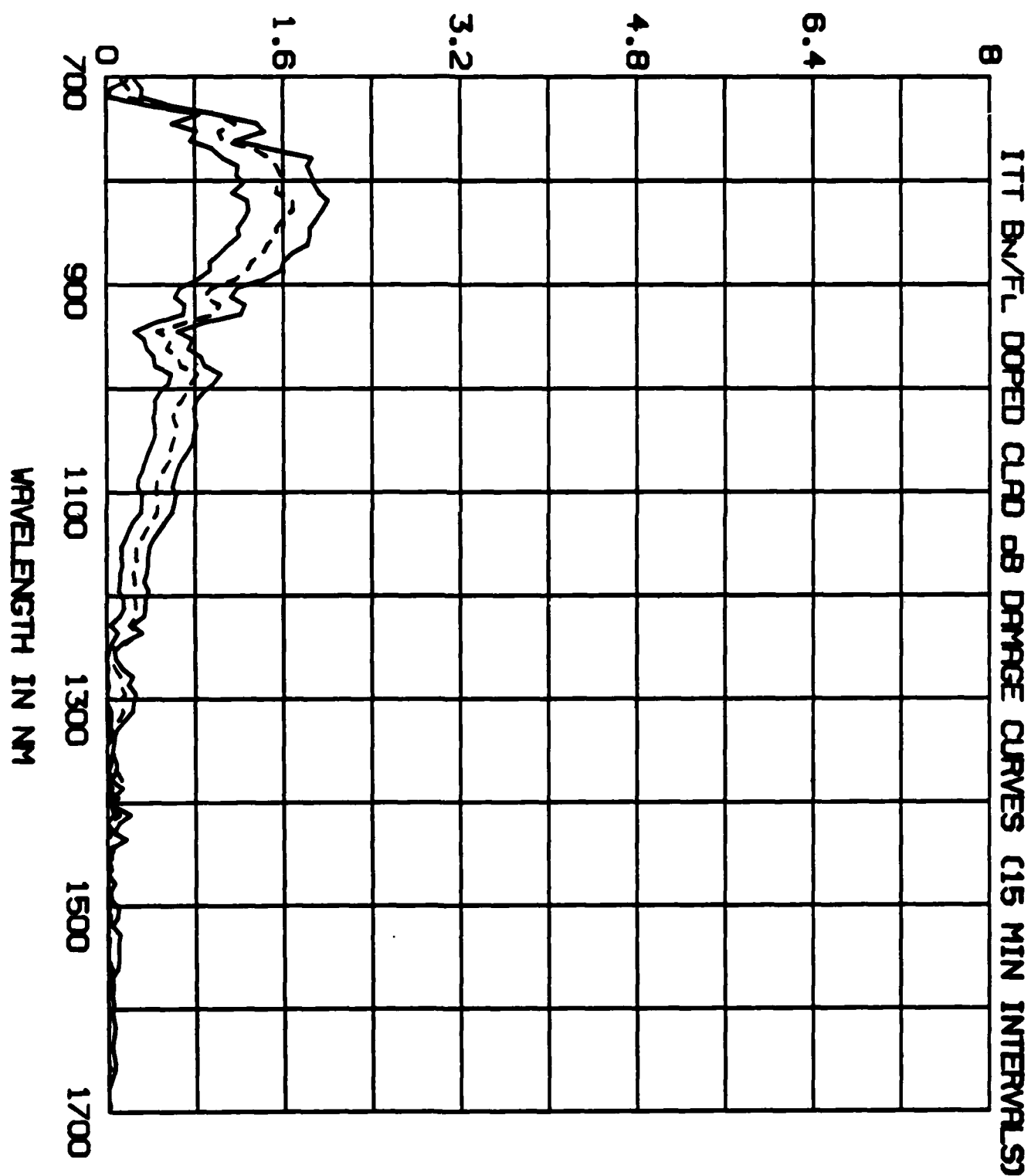
RADIATION INDUCED DAMAGE IN dB/KM

QUARTZ & SILICE dB DAMAGE CURVES(16 MIN INTERVALS)

WAVELENGTH IN NM

RAIATION INDUCED DAMAGE IN dB/KM

ITT SUPRASIL dB DAMAGE CURVES (15 MIN INTERVALS)

RADIATION INDUCED DAMAGE IN dB/KM

ITT Ge DOPED CLAD dB DAMAGE CURVES (15 MIN INTERVALS)

WAVELENGTH IN NM

RADIATION INDUCED DAMAGE IN dB/KM

ITT Bn/FL DOPED CLAD dB DAMAGE CURVES (15 MIN INTERVALS)

WAVELENGTH IN NM

CONCLUSIONS

Four fibers were studied in detail, with 50-100 meter lengths of fiber wound on a spool and mounted on the front of the neutron generator for the one-hour irradiation period. The fibers can be categorized into two general groups. The ITT Suprasil fiber and the Quartz & Silice fiber were very high purity silica core fibers. The other two fibers were ITT fibers and both were germanium doped silica core fibers. The primary difference between the two silica fibers was that the ITT Suprasil had a high water content in comparison with the Quartz & Silice fiber. The difference between the two doped core fibers is the doping utilized in the cladding.

The first, most important conclusion to be drawn from the data was the drastic decrease in the amount of radiation induced damage as the wavelength increased from 800 to 1100 nanometers. This trend is especially important if one is trying to create a system that is radiation hard.

Four secondary conclusions can also be drawn, but without a greater number of data runs, these conclusions cannot be confirmed. First, the high purity silica fibers seem to damage in relation to the amount of water present in the fiber. The high water content fiber (ITT Suprasil) had several dB less damage than the low water content (Quartz

& Silice).fiber. Second, the two high purity silica fibers
damaged much more heavily than the two doped silica fibers.
It was also noticed that the doped fiber with the boron-
fluorine doped cladding damaged more heavily than the doped
fiber with a germanium doped cladding. The last trend noted
was that all of the fibers showed a saturation of damage as
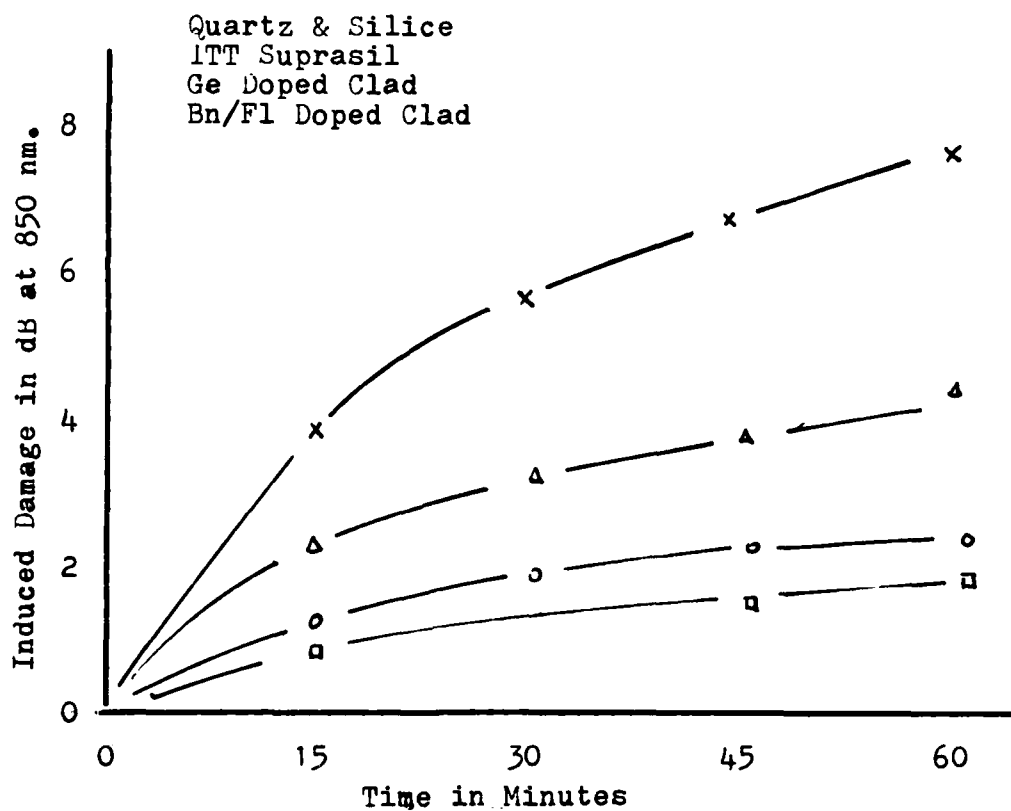the time of irradiation approached one hour (Figure #5).

Figure #5

Plot of Induced Damage Versus Time

A third result that merits further study was found in
the Quartz & Silice fiber recovery curves (Appendix #5).
These curves show that after forty-five minutes of recovery,
the fiber had a lower inherent loss than it did before the
radiation damaged it. This most startling result deserves
study in much greater detail.

DISCUSSION

The main conclusion, that the damage decreases with wavelength, can be understood using band theory. The broken bonds caused by the neutrons cause defect energy levels to exist in the energy gap. The energy of these levels is related to the type of trap which is formed when the bond is broken. Because the damage level drops off so rapidly in the 800 to 1100 nanometer range, one can generalize that the of the trapped holes and electrons correspond only to photons with higher energies (Ultraviolet and visible frequencies).

The secondary conclusions can also be understood using existing theories of solid state physics. The high water content fiber may damage less because of the presence of water near the broken bond. The water could ionize and the hydrogen ion may fill the dangling oxygen orbital, and the OH ion may fill the silicon's hole trap. This phenomenon would cause the defect energy levels to disappear, lessening the damage.

The saturation of the fiber with damage centers can also be easily understood. Assuming that the neutron-strained bond interaction is the main source of defects, it seems logical that there would only be a limited number of strained

bonds in the lattice. The other conclusions are not very easily understood, and with such a small data base, defin - tive explanations are impossible. The study of the radiation effects is by no means complete. Many more studies like this one must be completed before we can fully understand the damage phenomena.

ENDNOTES

[1] G. H. Sigel and E. J. Frieble, "Radiation Damage in Doped-Silica Fibers," an unpublished paper.

[2] Grant R. Fowles, Introduction to Modern Optics (New York: Holt, Rinehart and Winston, Inc., 1975), pp. 46-47.

[3] Personal interview with Dr. G.H. Sigel of the Naval Research Labratory, 21 April 1981.

[4] Charles Kittel, Introduction to Solid State Physics (New York: John Wiley & Sons, Inc., 1975), pp. 186-203.

[5] Sigel Interview.

[6] Stewart E. Miller and Alan G. Chynoweth, Optical Fiber Telecommunications (New York: Academic Press, 1979), pp. 164-170.
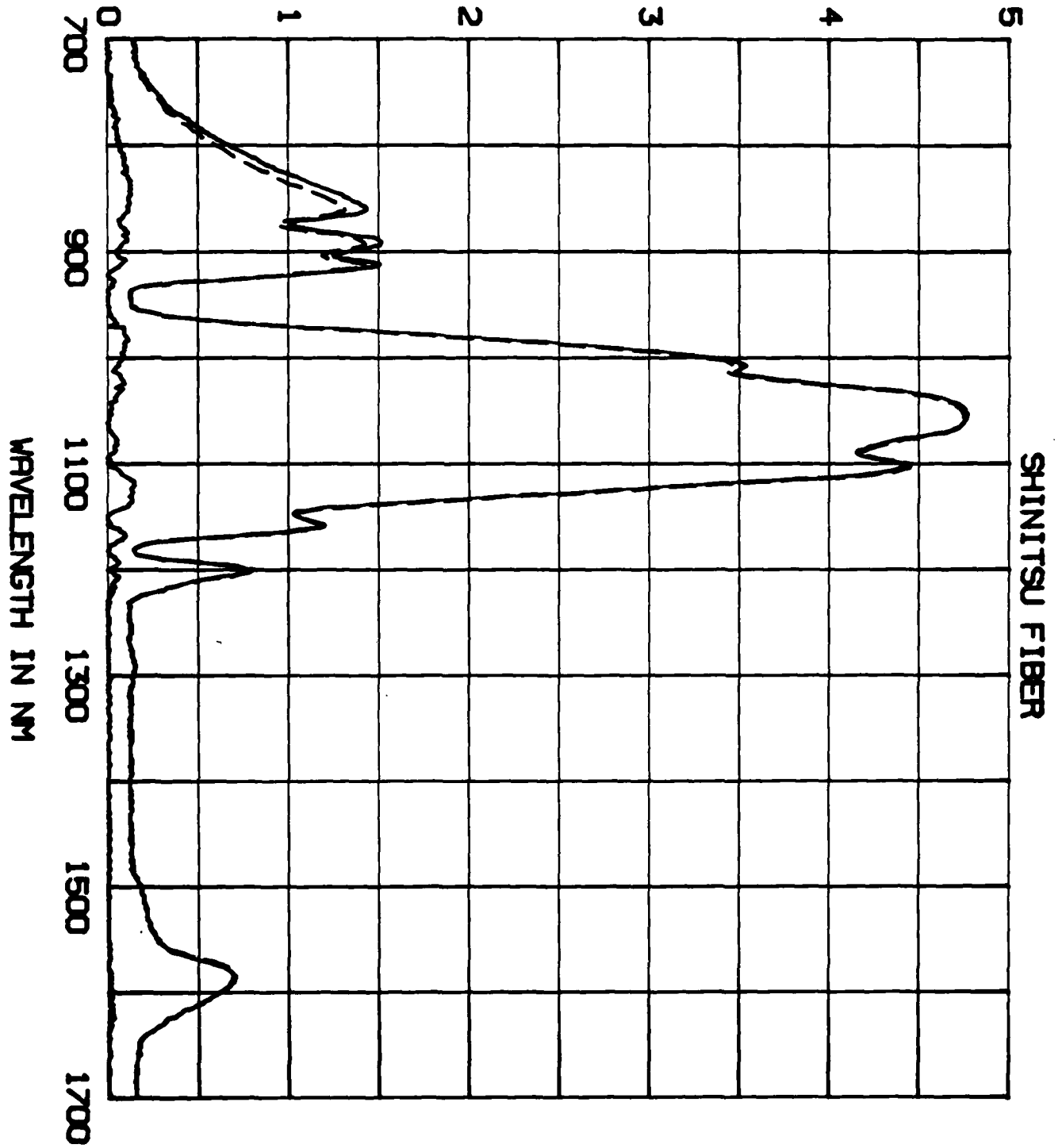
[7] "Radiation Damage in Doped-Silica Fibers."

A Selected Bibliography

Fowles, Grant R. Introduction to Modern Optics. New York:
  Holt, Rinehart and Winston, Inc., 1975.

Kittel, Charles. Introduction to Solid State Physics.
  New York: John Wiley & Sons, Inc., 1976.

Miller, Stewart E., and Alan G. Chynoweth. Optical Fiber
  Telecommunications. New York: Academic Press, 1979.

Sigel, G. H., and E. J. Friebele. Radiation Damage in Doped
  Silica Fibers. (Unpublished paper.)

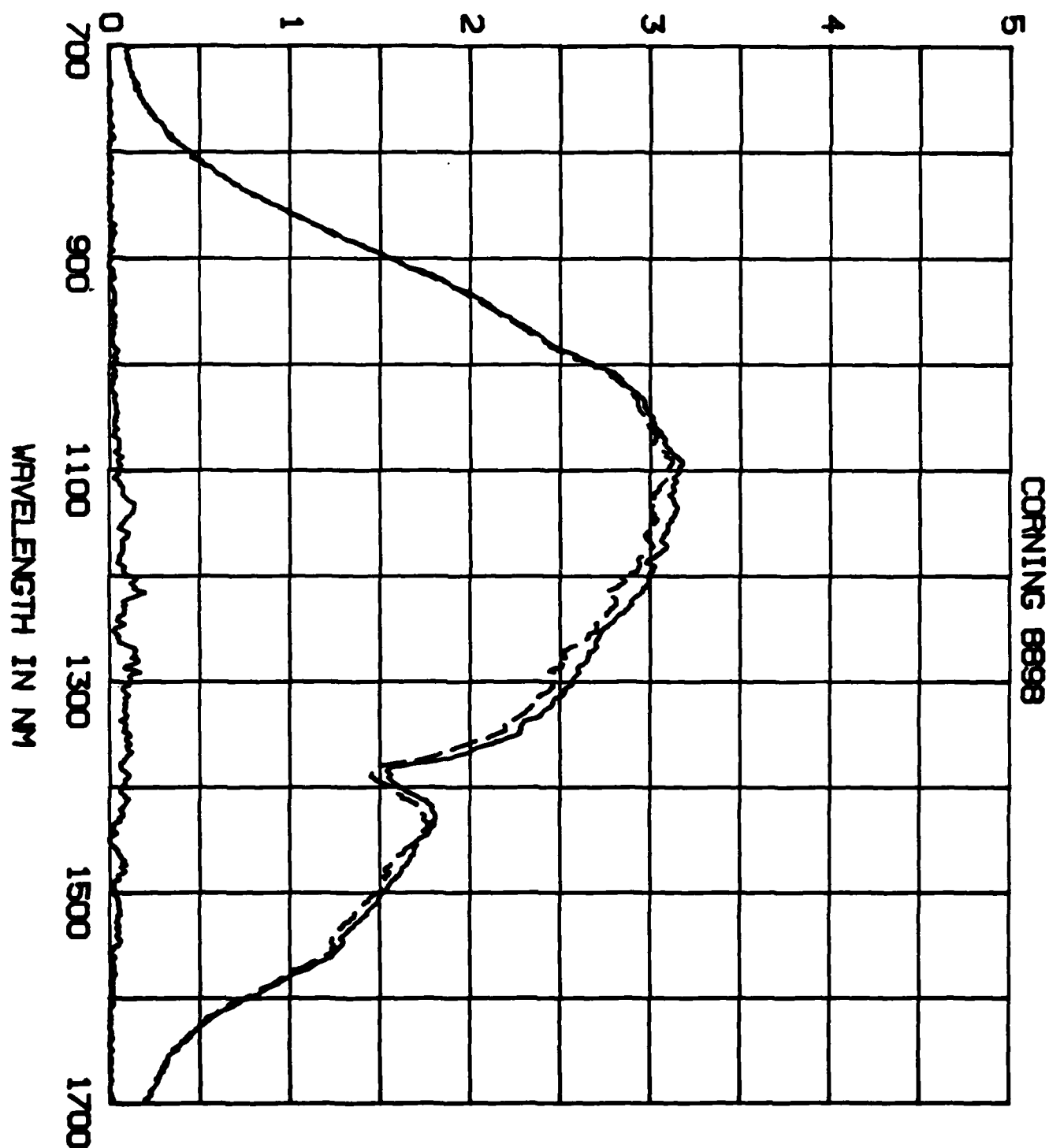Personal interview with Dr. G. H. Sigel, Washington D.C.,
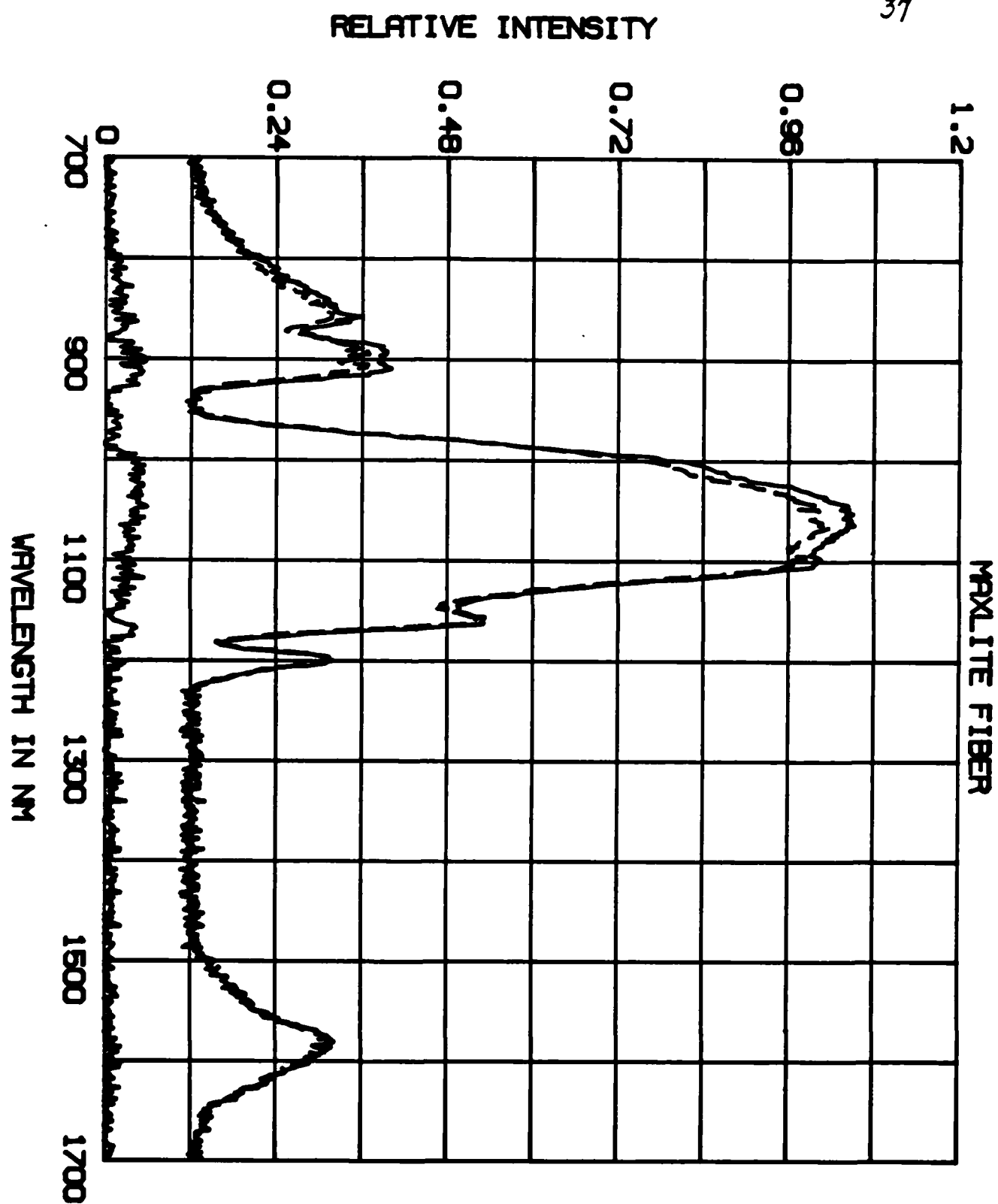 21 April 1981.

APPENDIX #1

   This section contains the result obtained in the initial
data runs. Each graph is for one fiber, and contains the
before and after irradiation runs, and plotted along the
bottom is plotted the difference between the two curves.
The difference between the curves is very slight, and the
noise destroys it completely, rendering this data unusable.

RELATIVE INTENSITY

SHINITSU FIBER

WAVELENGTH IN NM

RELATIVE INTENSITY

CORNING 8898

WAVELENGTH IN NM

37

RELATIVE INTENSITY

MAXLITE FIBER

WAVELENGTH IN NM

APPENDIX #2

The following graph is the intensity versus wavelength graph for the Quartz & Silice fiber. This curve is representative of the four fibers studied. The uppermost curve is the reference run, and the curves in descending order are the fifteen, thirty, forty-five and sixty minute runs. This graph, like the others, is not useful in the form it is in, but is included to represent the raw data.

RELATIVE INTENSITY

QUARTZ & SILICE RELATIVE INTENSITY CURVES (15 MIN INTERVALS)

WAVELENGTH IN NM
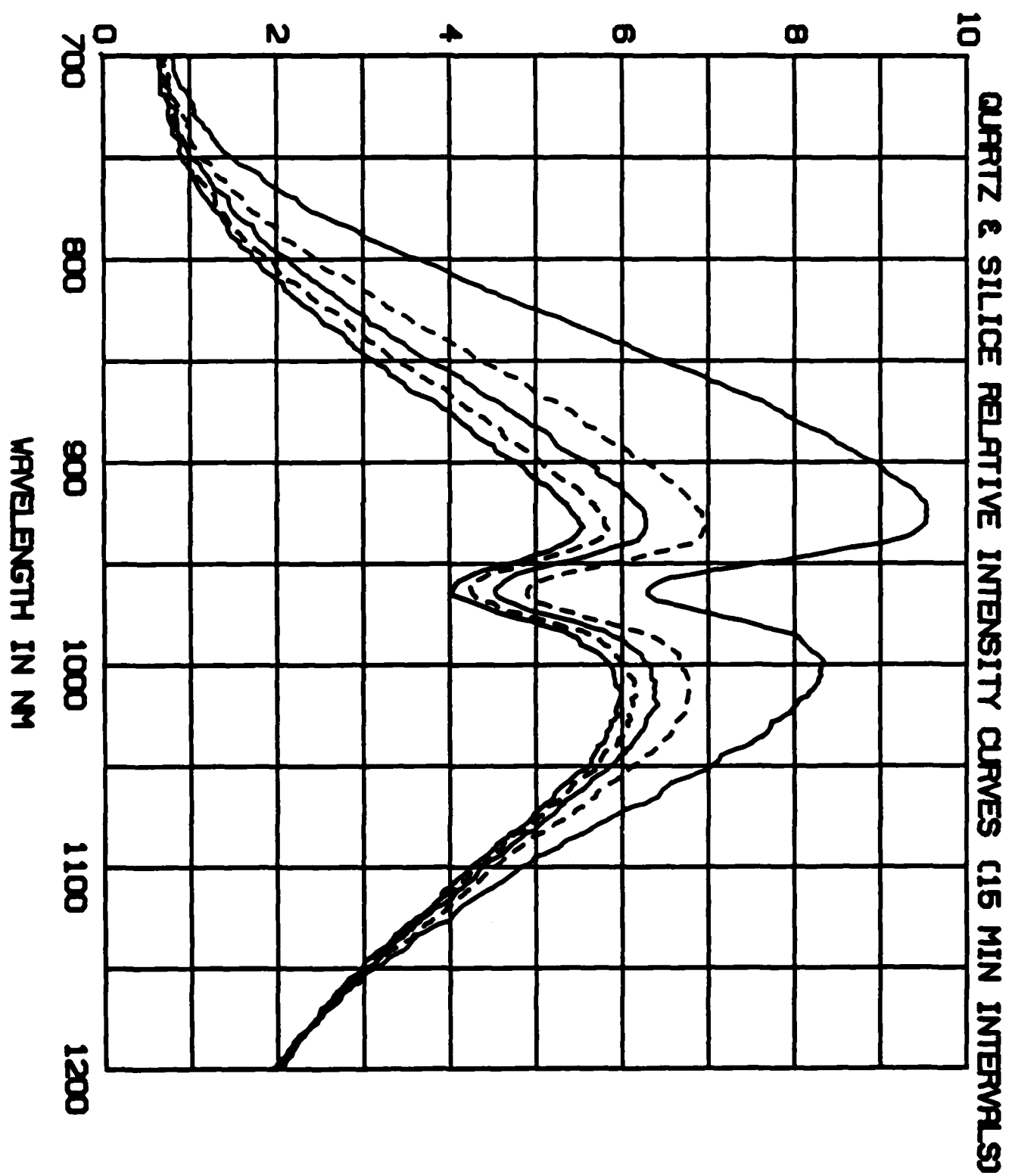
APPENDIX #3

This section contains the model and results of a computer study done to maximize the neutron flux through approximately 100 meters of fiber. The model is drawn below, and the computer program is listed with a table of results.
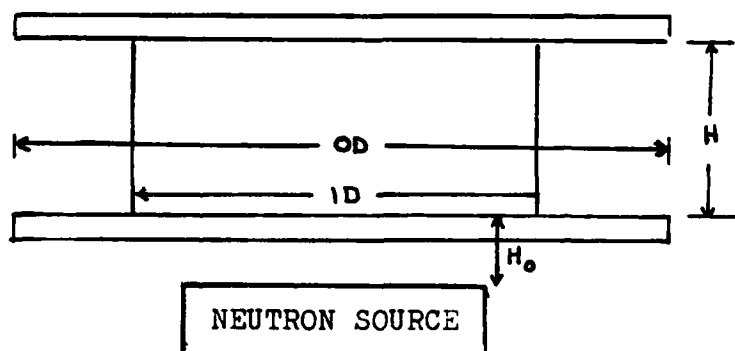
```
100 REM"A IS ID. B IS OD. C IS STEP SIZE"
110 PRINT "INPUT ID, OD, AND STEP SIZE IN CM";
120 INPUT A,B,C
125 FOR H=.2 TO 3 STEP .1
130 FOR D=(A+C/2) TO B STEP C
140 REM "E AND F ARE THE COORDINATES ON THE SOURCE"
150 FOR E=-1.85 TO 1.85 STEP .1
160 FOR F=-1.85 TO 1.85 STEP .1
170 REM "G IS THE DIST FROM SOURCE POINT TO INCREMENTAL AREA"
180 G=SQR((D-E)^2+F^2+H^2)
190 I=H/G
200 J=SQR(E*E+F*F)
210 IF J>1.85 THEN 290
220 REM "K IS CURRENT DENSITY FUNCTION"
230 K=1-(J/1.8545)^10
240 REM"L IS THE INCREMENTAL AREA"
250 L=((355/(113*360))*C*D)
260 REM"M IS COS()*AREA*FLUX/DIST^2 ,THE SOLID ANGLE"
270 M=I*L*K/G^2
280 N=N+M
290 NEXT F
300 NEXT E
310 REM"H IS THE AREA OF AN ANNULUS"
320 P=360*N
330 O=O+P
340 N=0
350 NEXT D
360 PRINT "THE SOLID ANGLE IS";O
365 I=I+O
370 O=0
380 NEXT H
390 PRINT (I/5)
400 END
```

TABULATION OF RESULTS

First Spool:
ID- 1.5 cm
OD- 3.0 cm
H - 1.0 cm
Area of integration- 63.6 cm^2
Total solid angle- 2726

Second Spool:
ID- 1.5 cm
OD- 2.0 cm
H - 3.8 cm
Area of integration- 65.7 cm^2
Total solid angle- 3472

Third Spool:
ID- 1.5 cm
OD- 2.5 cm
H - 1.7 cm
Area of integration- 62.5 cm^2
Total solid angle- 3446

Fourth Spool:
ID- 1.5
OD- 3.5
H - .67
Area of integration- 62.8 cm^2
Total solid angle- 1981

APPENDIX #4

The next page is a listing of the program used in the final data runs to step the stepper motor and to sample the data using the analog to digital converter.

```
80 D=0
85 DIM D(6)
90 PRINT "INPUT FILE NUMBER";
100 INPUT Z
110 FIND Z
120 PAGE
130 A$="0000"
140 A=0
150 T=1
160 L=0
170 I1=0
180 I2=0
190 DIM C(6)
200 C=1
210 CALL "BSETUP",A$,L,C
220 PRINT "CLOCKWISE (C) OR COUNTERCLOCKWISE(CC)";
230 INPUT X$
240 PRINT "NUMBER OF STEPS";
250 INPUT X
260 IF X$="C" THEN 360
270 B$="0FFFFFFF"              Stepper motor command
280 CALL "IOBCD",B$,I1,I2
290 FOR Z=1 TO X
300 B$="FFFFFFFF"
310 GOSUB 450
320 B$="0FFFFFFF"
330 GOSUB 450
340 NEXT Z
350 GO TO 220
360 B$="0F000000"
370 CALL "IOBCD",B$,I1,I2
380 FOR Y=1 TO X
390 B$="FF000000"
400 CALL "IOBCD",B$,I1,I2
402 CALL "A/D",D(Y),T          Analog to digital converter
410 B$="0F000000"                  command
420 CALL "IOBCD",B$,I1,I2
422 CALL "A/D",D(Y),T
430 NEXT Y
440 GO TO 270
450 CALL "IOBCD",B$,I1,I2
480 RETURN
```

APPENDIX #5

The following two graphs are the result of a study of the recovery of the Quartz & Silice fiber after one hour of irradiation. The first graph is in the form of the raw data and the second is in the form of the other final graphs. The scale is negative because the recovery is being measured, not the damage.

RELATIVE INTENSITY

QUARTZ & SILICE RECOVERY CURVES (15 MIN INTERVALS)

QUARTZ & SILICE dB RECOVERY CURVES (15 MIN INTERVALS)

RECOVERY IN dB/KM

WAVELENGTH IN NM